# (E) Sediment geochemistry

## chemical composition of common arenites

TABLE 2-6. Mean composition of principal sandstone classes and average sandstone (Pettijohn, 1963, p. 15).

| | Quartz arenite | Lithic arenite | Gray-Wacke | Arkose | Average sandstone A | Average sandstone B | Average sandstone C |
|---|---|---|---|---|---|---|---|
| $SiO_2$ | 95.4 | 66.1 | 66.7 | 77.1 | 78.66 | 84.86 | 77.6 |
| $Al_2O_3$ | 1.1 | 8.1 | 13.5 | 8.7 | 4.78 | 5.96 | 7.1 |
| $Fe_2O_3$ | 0.4 | 3.8 | 1.6 | 1.5 | 1.08 | 1.39 | 1.7 |
| FeO | 0.2 | 1.4 | 3.5 | 0.7 | 0.30 | 0.84 | 1.5 |
| MgO | 0.1 | 2.4 | 2.1 | 0.5 | 1.17 | 0.52 | 1.2 |
| CaO | 1.6 | 6.2 | 2.5 | 2.7 | 5.52 | 1.05 | 3.1 |
| $Na_2O$ | 0.1 | 0.9 | 2.9 | 1.5 | 0.45 | 0.76 | 1.2 |
| $K_2O$ | 0.2 | 1.3 | 2.0 | 2.8 | 1.32 | 1.16 | 1.3 |
| $H_2O+$ | 0.3 | 3.6 | 2.4 | 0.9 | 1.33 | 1.47 | 1.7 |
| $H_2O-$ | | 0.7 | 0.6 | | 0.31 | 0.27 | 0.4 |
| $TiO_2$ | 0.2 | 0.3 | 0.6 | 0.3 | 0.25 | 0.41 | 0.4 |
| $P_2O_5$ | | 0.1 | 0.2 | 0.1 | 0.08 | 0.06 | 0.1 |
| MnO | | 0.1 | 0.1 | 0.2 | trace | trace | 0.1 |
| $CO_2$ | 1.1 | 5.0 | 1.2 | 3.0 | 5.04 | 1.01 | 2.5 |
| $SO_3$ | | | 0.3 | | 0.07 | 0.09 | 0.1 |
| Cl | | | | | trace | trace | trace |
| F | | | | | | | trace |
| S | | | 0.1 | | | | trace |
| BaO | | | | | 0.05 | 0.01 | trace |
| SrO | | | | | trace | none | trace |
| C | | | 0.1 | | | | trace |
| Ignition Loss | | | | | | | |
| Total | 100.7 | 100.0 | 100.4 | 100.0 | 100.41 | 99.86 | 100.0 |

A. Composite analysis of 253 sandstones.
B. Composite analysis of 371 sandstones used for building purposes.
C. Computed by taking 26 parts average graywacke, 25 parts average lithic arenite, 15 parts average arkose, and 34 parts average quartz arenite.

Pettijohn et al. 1987 p.59



## classification based on geochemistry

Herron 1988

Pettijohn 1963, 1987

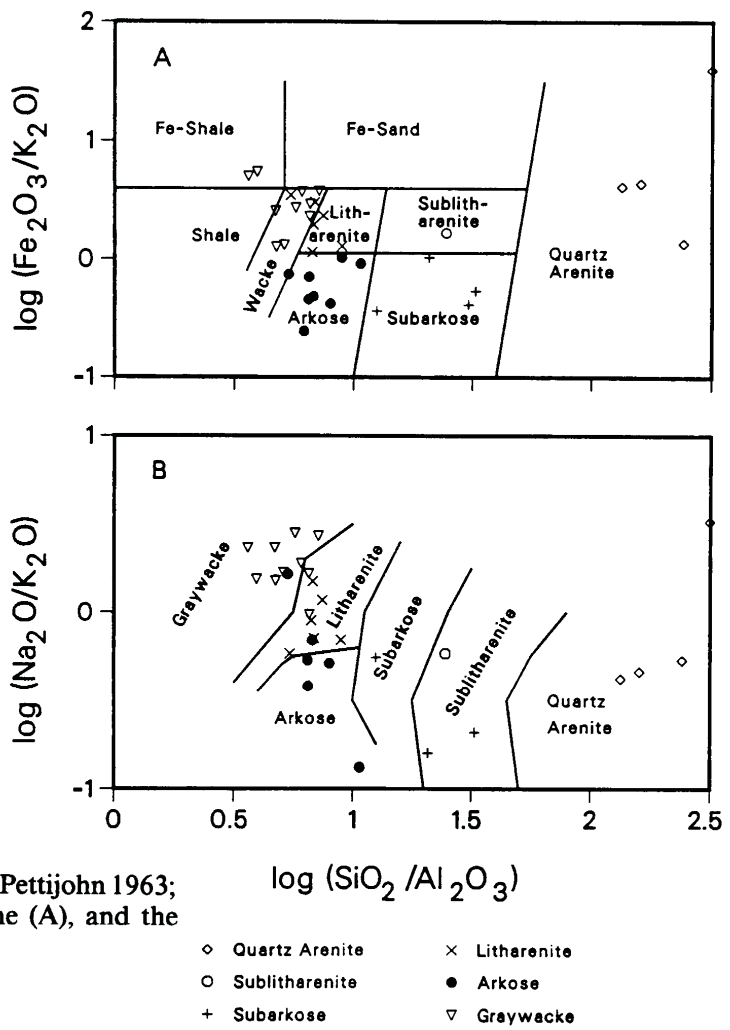


FIG. 3.—Benchmark sandstone chemical compositions (Pettijohn 1963; Pettijohn et al. 1972) plotted for the SandClass scheme (A), and the Pettijohn scheme (B).

## Example:

## Swiss Molasse Basin

1.

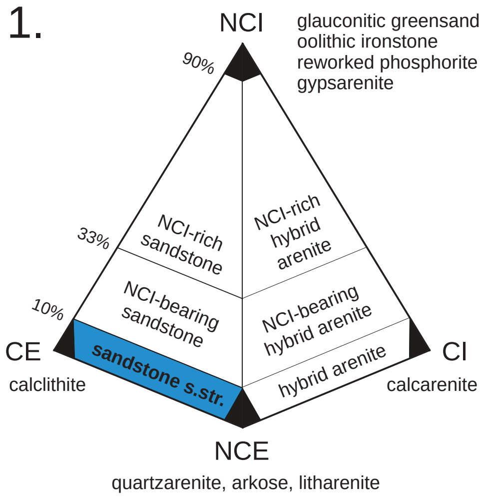


2.

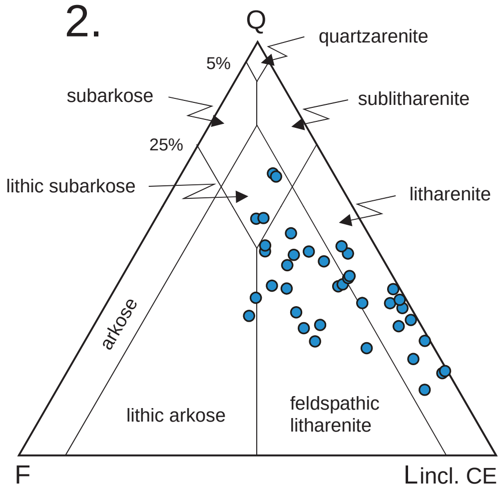


classification based on petrography

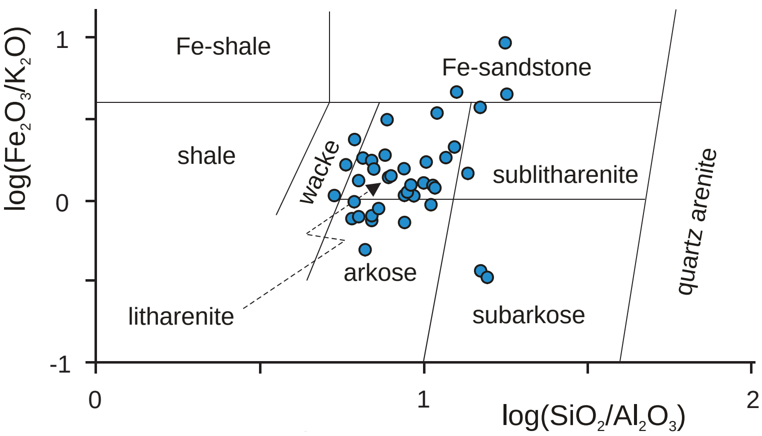


classification based on geochemistry

**TABLE 2-7. Average chemical composition of sandstones of various tectonic settings (after Bhatia, 1983, Table 10).**

| | Oceanic island arc | Continental island arc | Active continental margin | Passive margin |
|---|---|---|---|---|
| $SiO_2$ | 58.83 | 70.69 | 73.86 | 81.95 |
| $TiO_2$ | 1.06 | 0.64 | 0.46 | 0.49 |
| $Al_2O_3$ | 17.11 | 14.04 | 12.89 | 8.41 |
| $Fe_2O_3$ | 1.95 | 1.43 | 1.30 | 1.32 |
| FeO | 5.52 | 3.05 | 1.58 | 1.76 |
| MnO | 0.15 | 0.10 | 0.10 | 0.05 |
| MgO | 3.65 | 1.97 | 1.23 | 1.39 |
| CaO | 5.83 | 2.68 | 2.48 | 1.89 |
| $Na_2O$ | 4.10 | 3.12 | 2.77 | 1.07 |
| $K_2O$ | 1.60 | 1.89 | 2.90 | 1.71 |
| $P_2O_5$ | 0.26 | 0.16 | 0.09 | 0.12 |
| $Fe_2O_3$* + MgO | 11.73 | 6.79 | 4.63 | 2.89 |
| $Al_2O_3/SiO_2$ | 0.29 | 0.20 | 0.18 | 0.10 |
| $K_2O/Na_2O$ | 0.39 | 0.61 | 0.99 | 1.60 |
| $Al_2O_3/(CaO + Na_2O)$ | 1.72 | 2.42 | 2.56 | 4.15 |

All averages on volatile-free basis.
* Total iron as $Fe_2O_3$.

Pettijohn et al. 1987 p.59

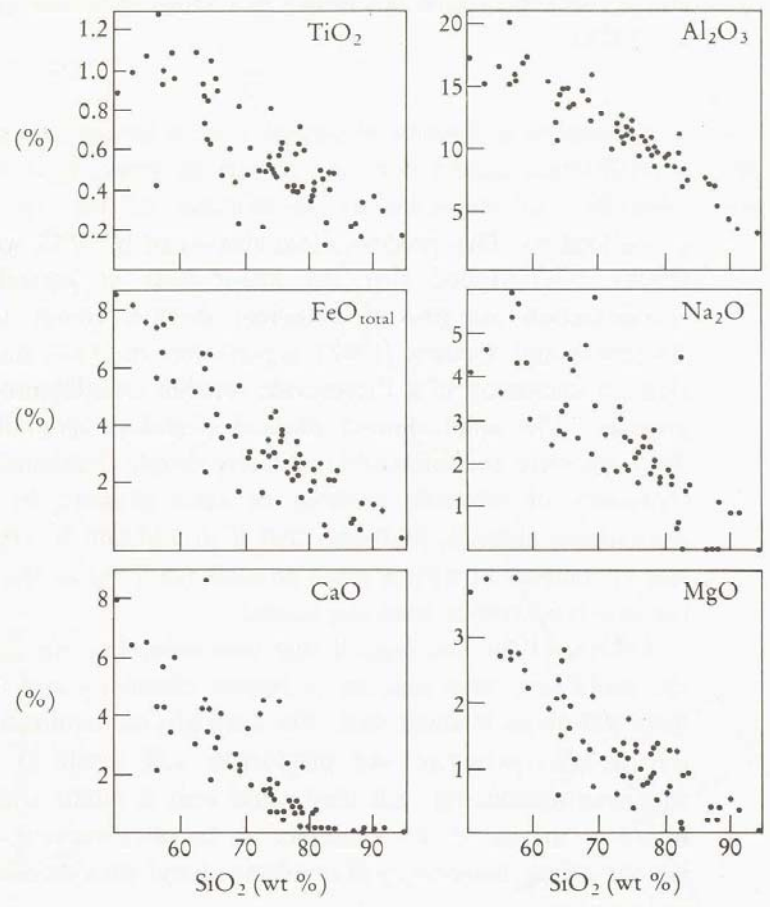


Rollinson 1993

Harker variation diagrams for quartz-rich sandstone suites from eastern Australia (after Bhatia, 1983). The increase in $SiO_2$ reflects an increased mineralogical maturity, i.e. a greater quartz content and a smaller proportion of detrital grains.

# *Tectonic Setting* – Discrimination diagrams

## (1) Major elements:

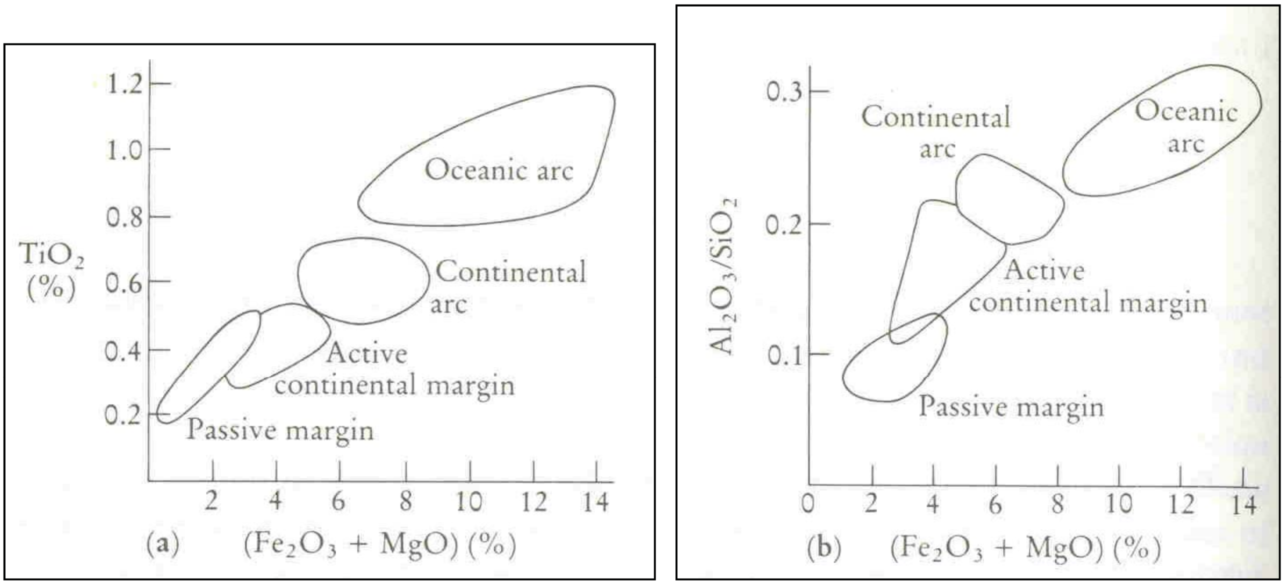


Discrimination diagrams for sandstones (after Bhatia, 1983), based upon (a) a bivariate plot of $TiO_2$ vs ($Fe_2O_{3(tot)}$ + MgO) and (b) a bivariate plot of $Al_2O_3/SiO_2$ vs ($Fe_2O_{3(tot)}$ + MgO). The fields are oceanic island-arc, continental island-arc, active continental margin and passive margin.

Rollinson 1993 p.208

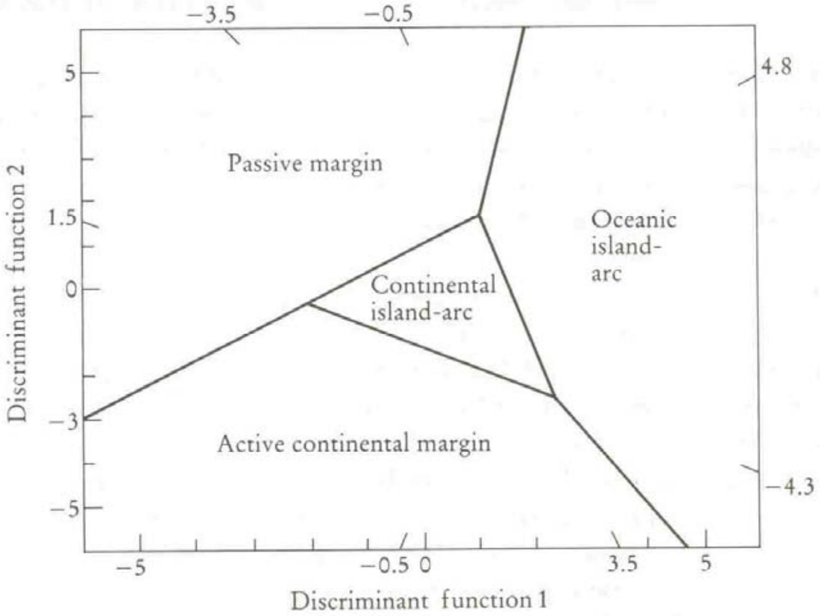


Rollinson 1993 p.207

The discriminant function diagram for sandstones (after Bhatia, 1983), showing fields for sandstones from passive continental margins, oceanic island-arcs, continental island-arcs and active continental margins. The discriminant functions are as follows:

$$\text{Discriminant function 1} = -0.0447\,SiO_2 - 0.972\,TiO_2 + 0.008\,Al_2O_3 - 0.267\,Fe_2O_3 + 0.208\,FeO - 3.082\,MnO + 0.140\,MgO + 0.195\,CaO + 0.719\,Na_2O - 0.032\,K_2O + 7.510\,P_2O_5 + 0.303$$

$$\text{Discriminant function 2} = -0.421\,SiO_2 + 1.988\,TiO_2 - 0.526\,Al_2O_3 - 0.551\,Fe_2O_3 - 1.610\,FeO + 2.720\,MnO + 0.881\,MgO - 0.907\,CaO - 0.177\,Na_2O - 1.840\,K_2O + 7.244\,P_2O_5 + 43.57$$

(from Bhatia, 1983 — Table 3). The plotting coordinates are extracted from Bhatia (1983 — Figure 7).



## discrimination of tectonic setting by major elements

## does it work properly ?

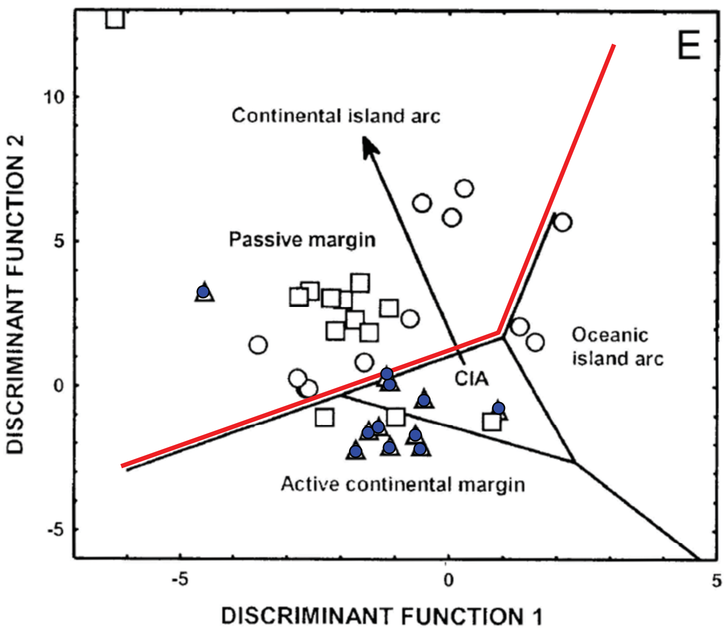


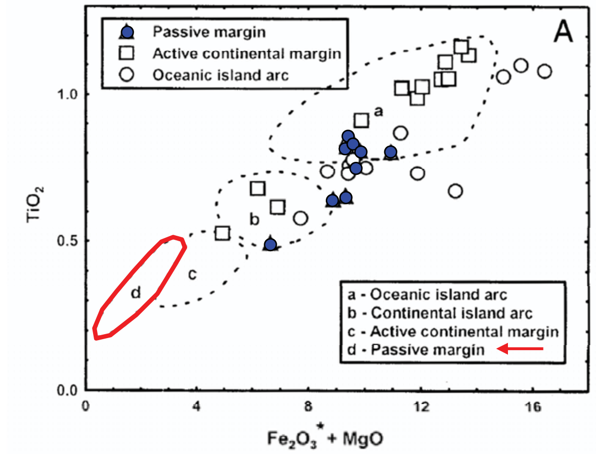


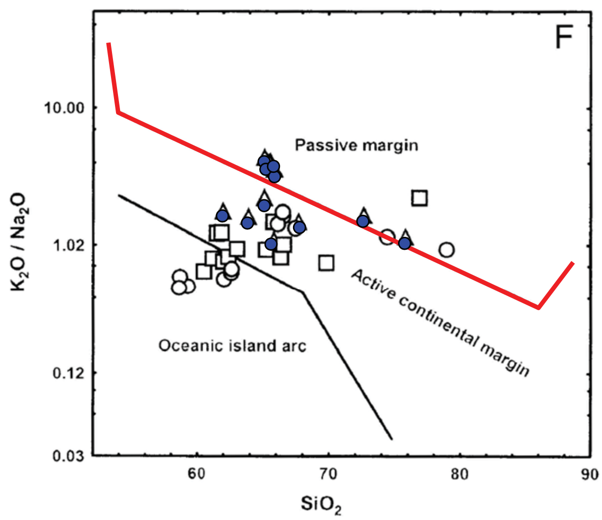


*Armstron-Altrin & Verma 2005, Sed Geol 177*

## success rate

| This study | | | Inferred tectonic setting | | | | | |
|---|---|---|---|---|---|---|---|---|
| Figure # | Known tectonic setting | # of averages | PM | ACM | CIA | OIA | Outside any field | Percent (%) success |
| | | | # of averages plotting in a given field (defined by Bhatia, 1983) | | | | | |
| Fig. 5A | PM | **11** | **0** | 0 | 1 | 6 | 4 | → 0 |
| | ACM | **13** | 0 | **1** | 2 | 9 | 1 | 7.7 |
| | OIA | **12** | 0 | 0 | 1 | **2** | 9 | 16.7 |
| Fig. 5B | PM | **11** | **0** | 0 | 0 | 0 | 11 | → 0 |
| | ACM | **13** | 0 | **1** | 1 | 0 | 11 | 7.7 |
| | OIA | **12** | 0 | 0 | 0 | **0** | 12 | 0 |
| Fig. 5C | PM | **11** | **0** | 1 | 0 | 3 | 7 | → 0 |
| | ACM | **13** | 0 | **1** | 1 | 9 | 2 | 7.7 |
| | OIA | **12** | 0 | 0 | 0 | **7** | 5 | 58.3 |
| Fig. 5D | PM | **11** | **0** | 0 | 0 | 8 | 3 | → 0 |
| | ACM | **13** | 0 | **1** | 1 | 0 | 11 | 7.7 |
| | OIA | **12** | 0 | 0 | 0 | **3** | 9 | 25 |
| Fig. 5E | PM | **11** | **1** | 6 | 4 | 0 | 0 | → 9.1 |
| | ACM | **13** | 9 | **2** | 1 | 0 | 1 | 15.4 |
| | OIA | **12** | 9 | 0 | 0 | **3** | 0 | 25 |
| | | | # of averages plotting in a given field (defined by Roser and Korsch, 1986) | | | | | |
| Fig. 5F | PM | **11** | **6** | 5 | – | 0 | 0 | 54.5 |
| | ACM | **13** | 1 | **8** | – | 4 | 0 | 61.5 |
| | OIA | **12** | 2 | 4 | – | **6** | 0 | 50 |

*Armstron-Altrin & Verma 2005*

**→ be very careful with such discrimination diagrams !!!**



## the problem of grain-size

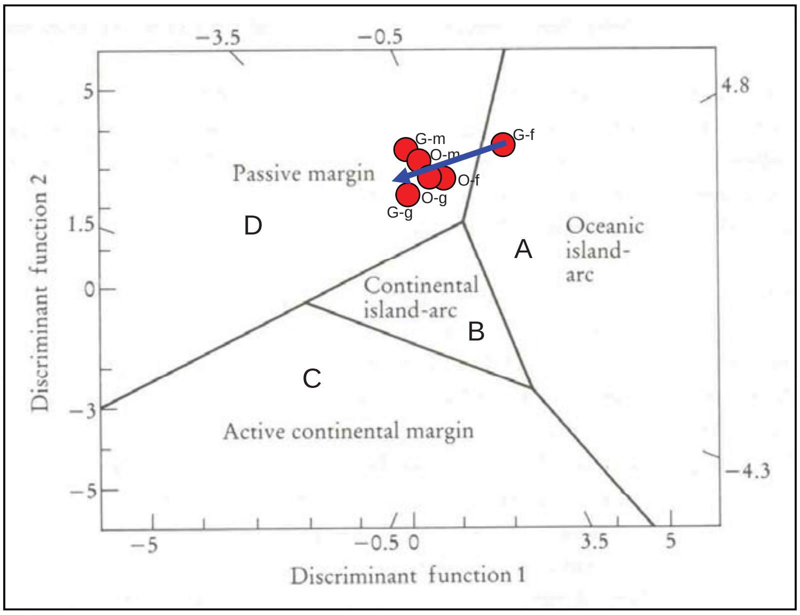


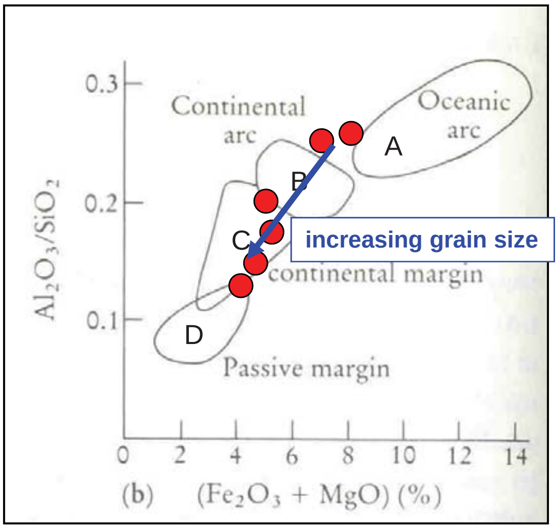


*Bhatia 1983, Bhatia & Crook 1986, Roser & Korsch 1988*

**greywackes from type-locality “Oberharzer Grauwacke“**

## Bivariate Ca / Mg / LOI-plots of Swiss Molasse sandstones (litharenites)

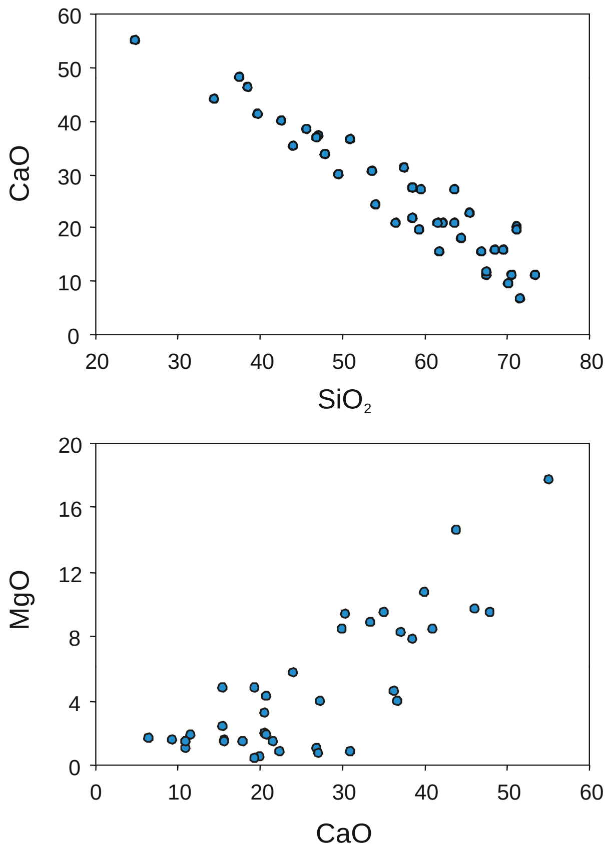


HvE - Sedimentpetrologie

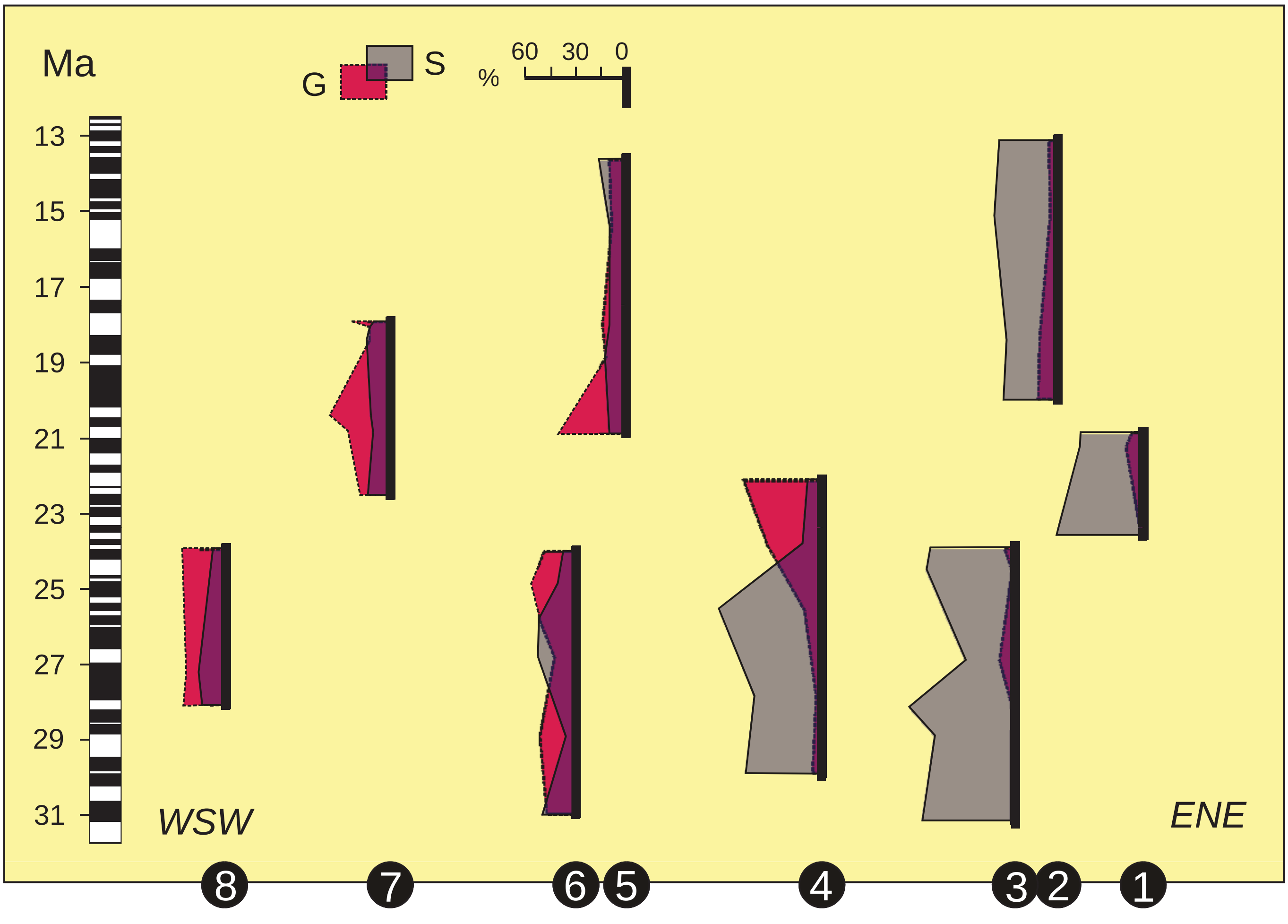


HvE - Sedimentpetrologie

# framework composition vs. wr-geochemistry

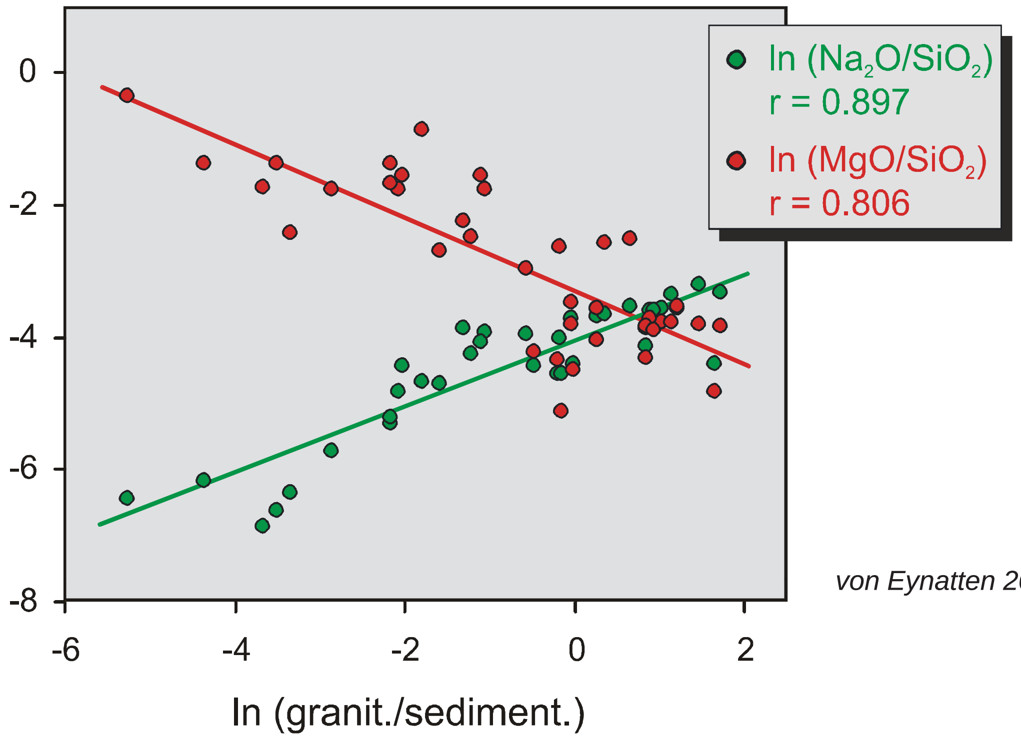


*von Eynatten 2003*



## (2) Trace elements:

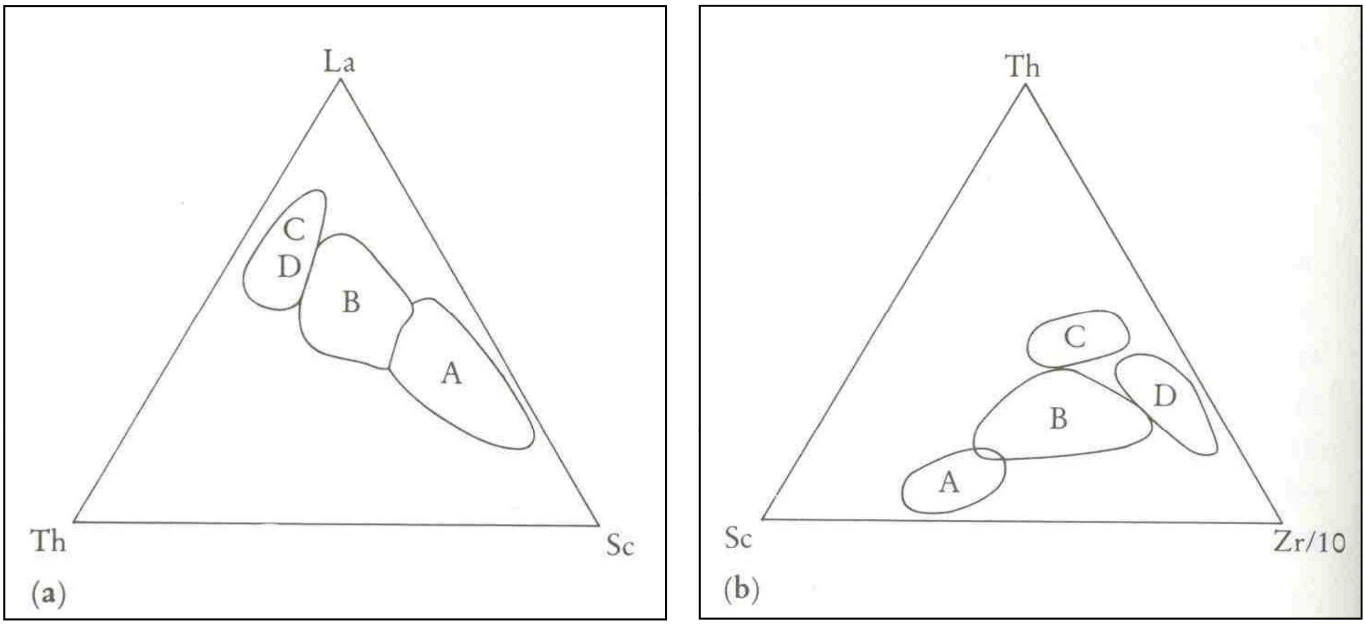


(a) La–Th–Sc discrimination diagram for greywackes; (b) Th–Sc–Zr/10 discrimination diagram for greywackes (after Bhatia and Crook, 1986). The fields are: A, oceanic island-arc; B, continental island-arc; C, active continental margin; D, passive margin.

Rollinson 1993 p.208

detection of various processes such as recycling, sorting, etc.

Th/Sc monitors the compositional variation of the source area, and Zr/Sc monitors zircon enrichment due to sedimentary (sorting and) recycling

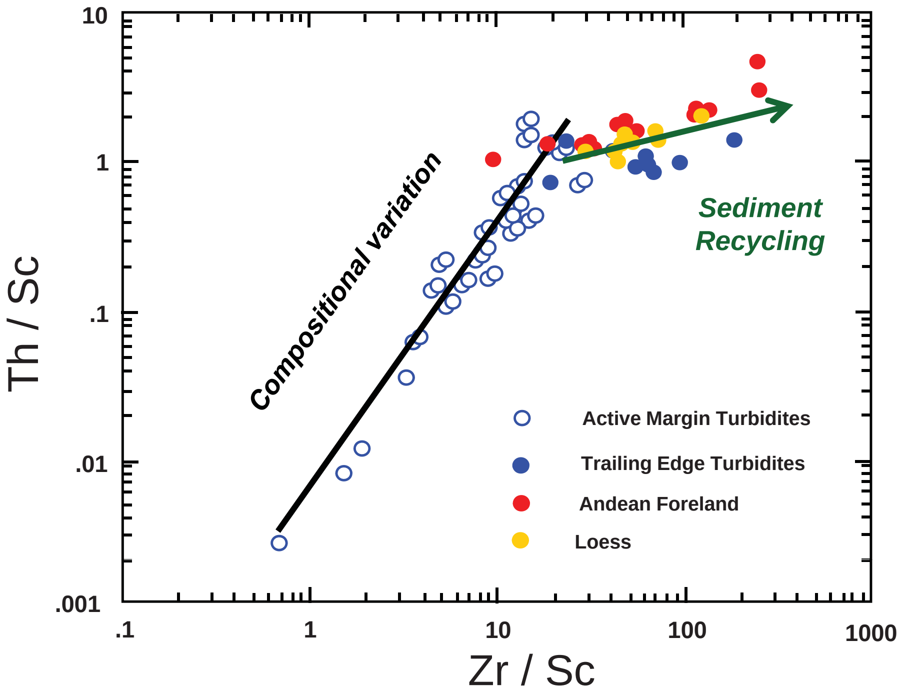


*McLennan 1993, GSA Spec Pap 284*



## Cr-spinel chemistry

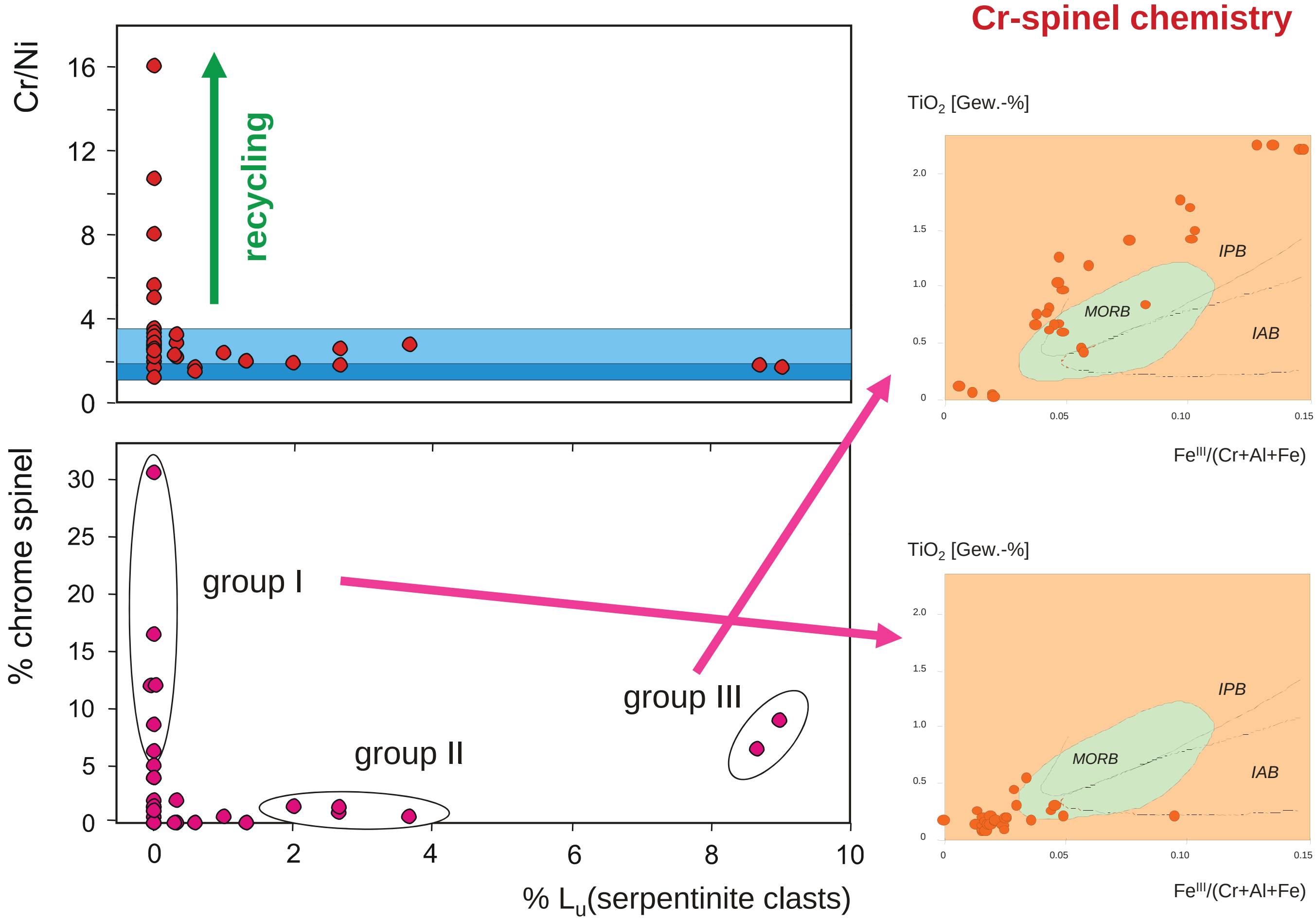


*von Eynatten 2003, Sedimentology 50*

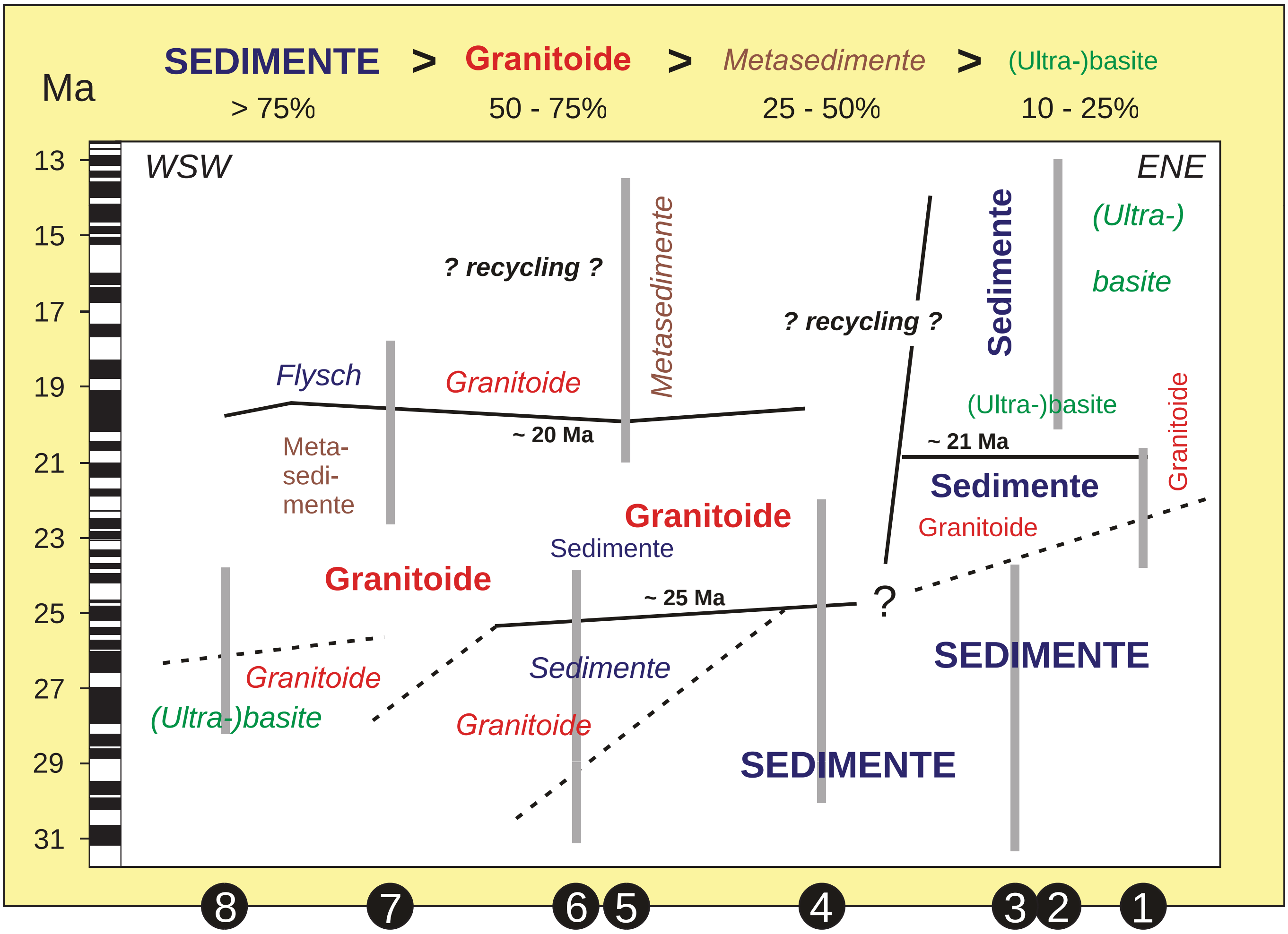


HvE - Sedimentpetrologie

von Eynatten 2003

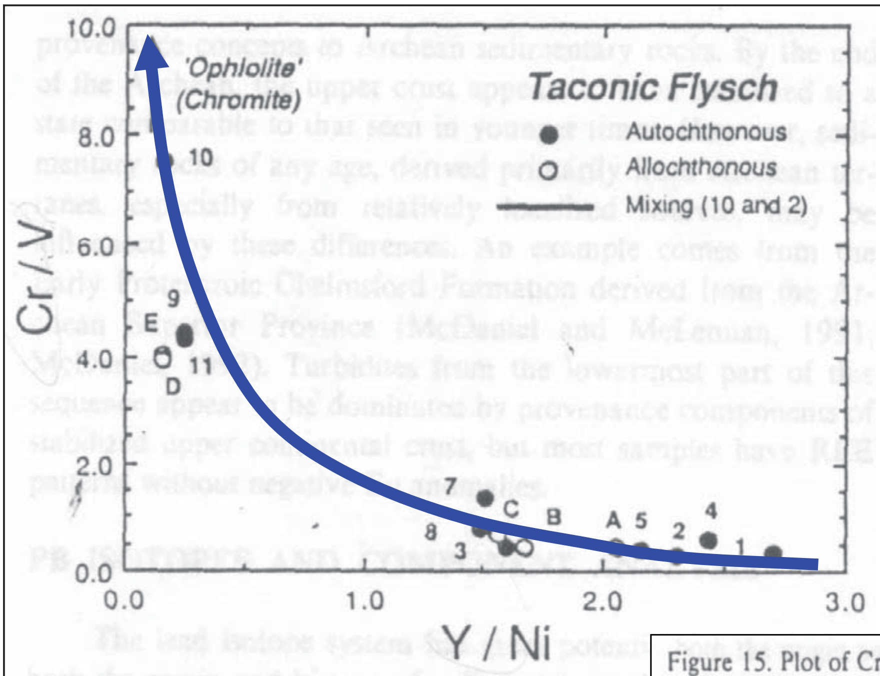


Contribution of mafic to ultramafic (ophiolitic) source rocks
**( Mixing! )**

*McLennan 1993*

Figure 15. Plot of Cr/V versus Y/Ni for early Paleozoic Taconic flysch from eastern North America illustrating the greater importance of an ophiolitic provenance as one moves north. Higher numbers and letters indicate more northerly outcrops. Each data point represents the average of several analyses from one formation/area. Also shown is a mixing line generated from the two data points with the lowest and highest Cr abundances. The Cr/V ratio is an index of the enrichment of Cr over the other ferromagnesian trace elements, whereas Y/Ni monitors the general level of ferromagnesian trace elements (Ni) compared to a proxy for HREE (Y). Mafic-ultramafic sources tend to have high ferromagnesian abundances; such a provenance would result in a decrease in Y/Ni. A mineral such as chromite, important in ophiolitic sequences, tends to concentrate Cr preferentially over other ferromagnesian elements. Data from Hiscott (1984).

HvE - Sedimentpetrologie

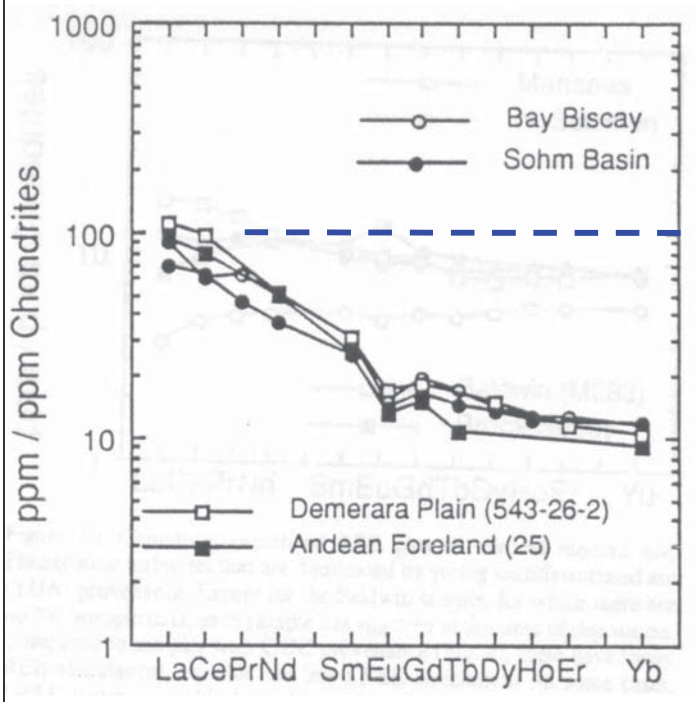


Figure 8. Chondrite-normalized REE plot of selected modern sediments that have an old upper continental crustal (OUC) provenance. The $\epsilon_{Nd}$ for each of these samples is less than −10. Note the similarity of the patterns with LREE enrichment, fairly flat HREE (i.e., $Gd_N/Yb_N$ = 1.0 to 2.0) and the negative Eu anomaly, characteristic of the upper continental crust. Data from White et al. (1985), McLennan et al. (1990), and Basu et al. (1990).

## Rare earth patterns of sediments from different sources

*McLennan 1993*

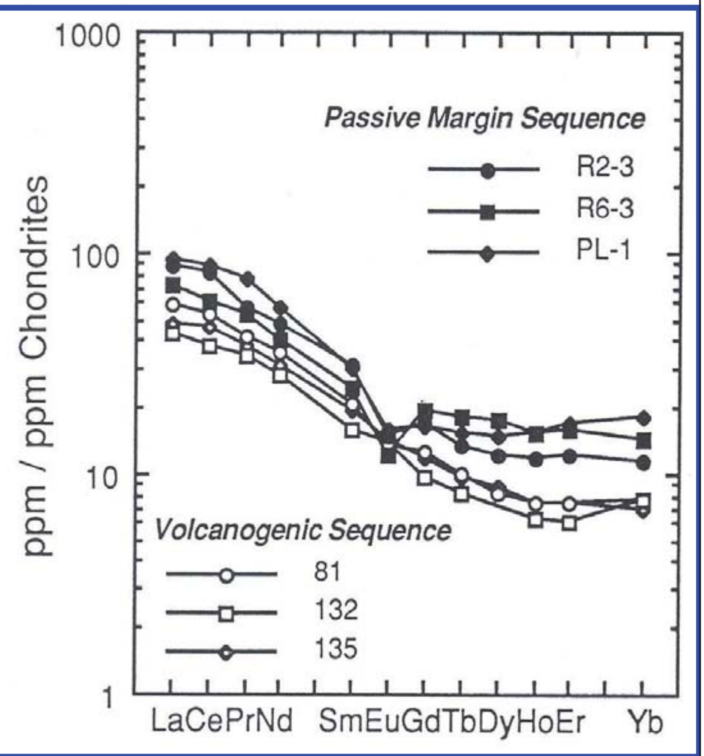




## Alteration
## (weathering, diagenesis, ...)

**Chemical Index of Alteration:**

$$CIA = 100 \frac{Al_2O_3}{Al_2O_3 + CaO^* + Na_2O + K_2O}$$

(with CaO* = CaO from silicate phases)

FIG. 1.—Changes in the volume percentages of minerals (ordinate) as a function of weathering intensity (measured by CIA, see Nesbitt and Young 1982, 1984) in the Stone Mountain weathering profile (Georgia, USA). Data are recalculated from results given by Grant (1963, fig. 1), and CIA values were calculated by noting the proportions of minerals and their respective CIA values (feldspars and biotite = 50; muscovite and illite = 75; kaolinite = 100).

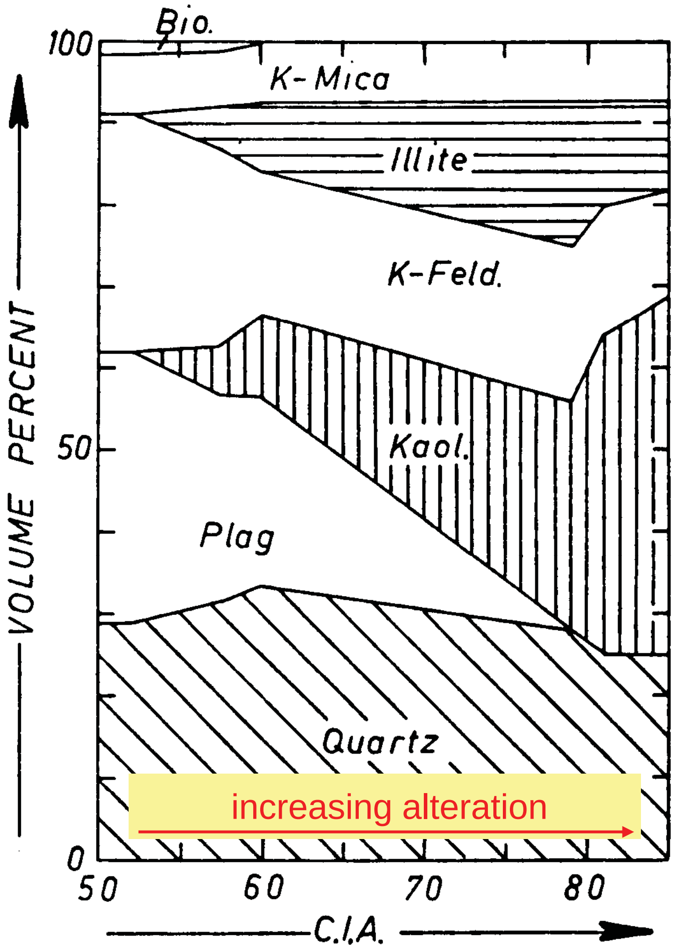


Nesbitt & Young 1989

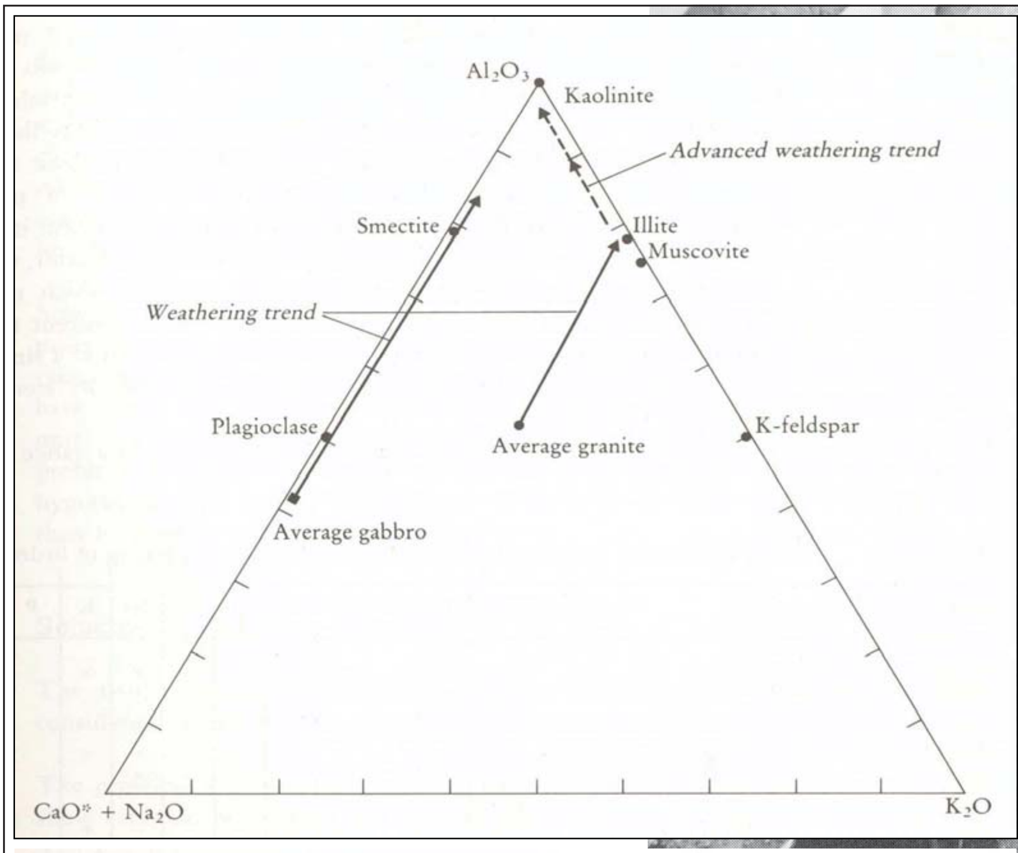


The $(Na_2O + CaO) - Al_2O_3 - K_2O$ diagram of Nesbitt and Young (1984, 1989) showing the weathering trends for average granite and average gabbro. The advanced weathering trend for granite is also shown. Compositions are plotted as molar proportions and the compositions of plagioclase, K-feldspar, muscovite and kaolinite are shown. CaO* represents the CaO associated with the silicate fraction of the sample.

Leeder 1999



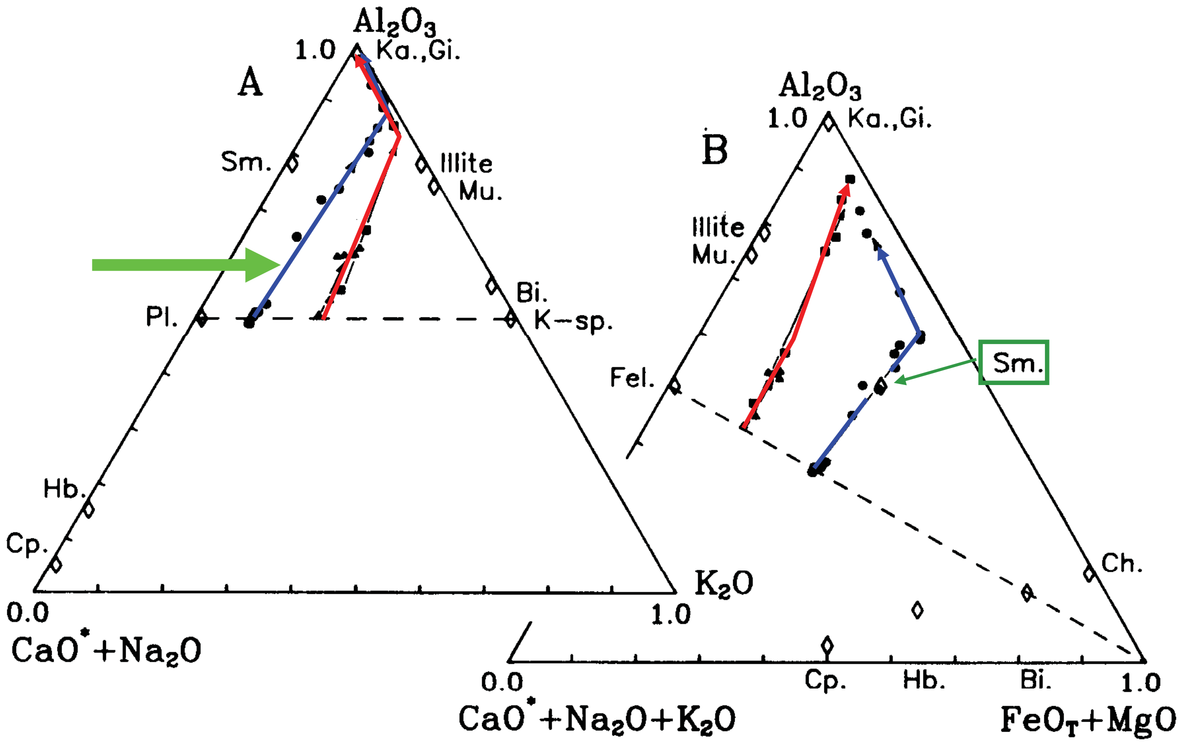


FIG. 4.—Weathering trends for the Mazaruni Granite profile (squares), the Ricany Granite profile (triangles), and the Toorongo Granodiorite profile (dots) are shown. The arrows in 4*A* (A-CN-K diagram) have been calculated from feldspar leach rate data. The arrows of 4*B* (A-CNK-FM diagram) are drawn to reflect the plotted data only. The diamonds represent idealized mineral compositions; Sm = smectite (montmorillonites and beidellites); Il = illite (sericites, phengites, celadonites); Bi = biotite; Fs = feldspars (plagioclase and K-feldspar). See figure 3 for other abbreviations. These triangular plots and all subsequent triangular plots are as MOLAR PROPORTIONS

Nesbitt & Young 1989

## chemical weathering of granitoid rocks

Toorongo granodiorite
(Nesbitt et al. 1980, GCA 44)

Chemical Index of Alteration:

$$100 \frac{Al_2O_3+CaO^*+Na_2O+K_2O}{Al_2O_3}$$

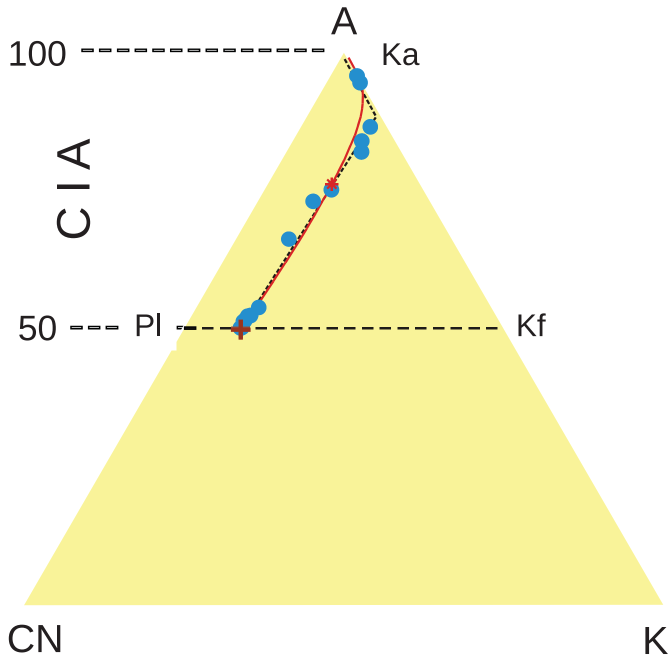




## chemical weathering of granitoid rocks

Toorongo
granodiorite

$s_k = (k \otimes p_{w1}) \oplus g$

$p_{w1} = (0.49, 0.13, 0.38)$
99.5%

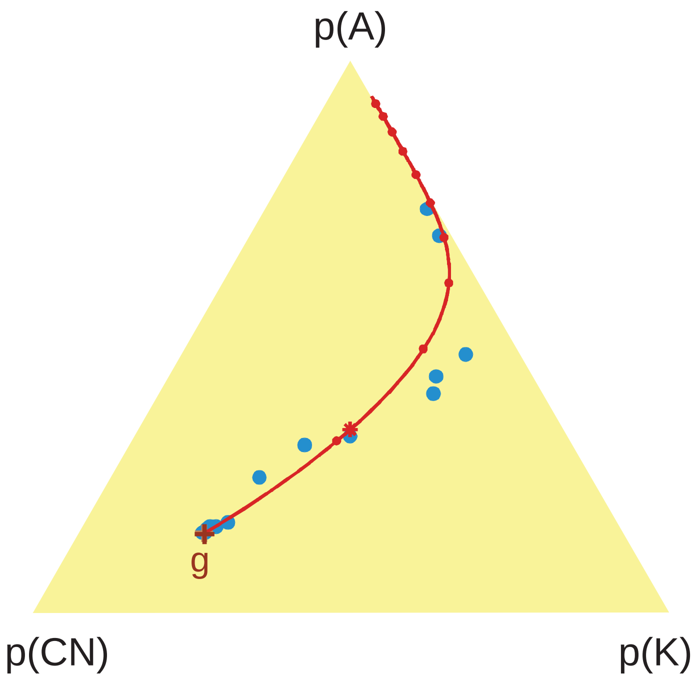


*von Eynatten et al. 2003*

# chemical weathering of granitoid rocks

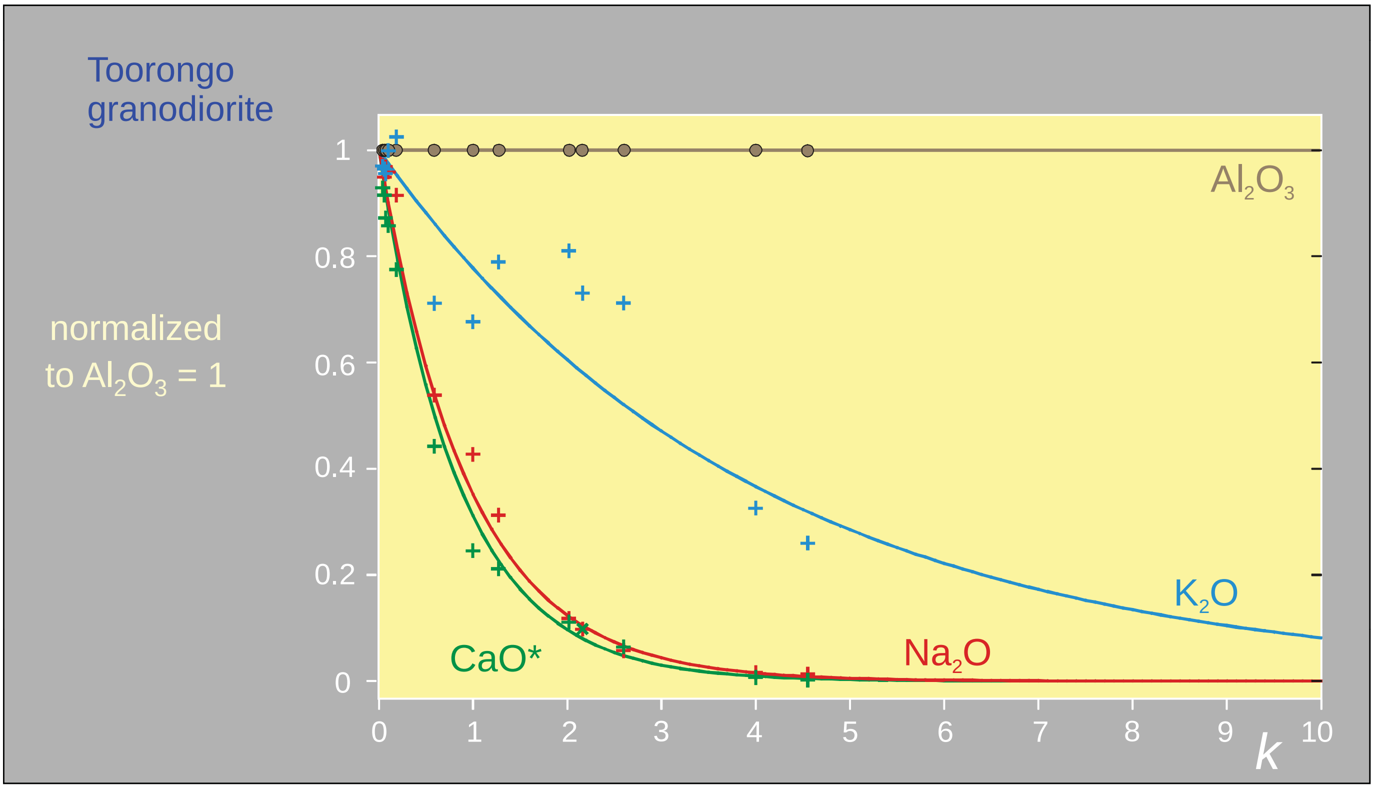


*von Eynatten et al. 2002, Math. Geol. 34*



# chemical weathering at global scales

*suspended sediment load of the world´s major rivers (McLennan 1993, J. Geol. 101)*

$s = cc \oplus (k \otimes p_{w2})$

$p_{w2} = (0.51, 0.13, 0.36)$
97.1%

$p_{w1} = (0.49, 0.13, 0.38)$
99.5%

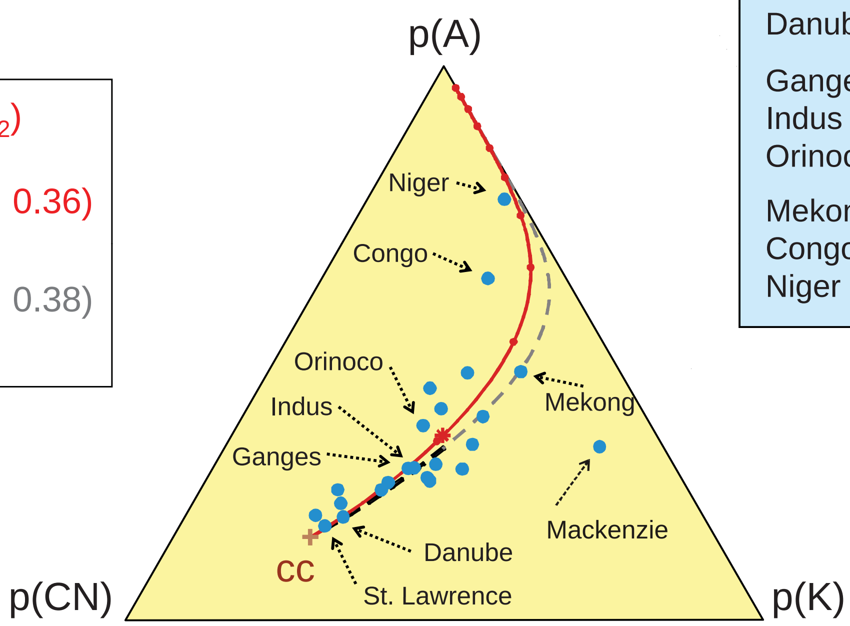


| ***river*** | ***k*** |
|---|---|
| St. Lawrence | 0.13 |
| Danube | 0.25 |
| Ganges | 0.75 |
| Indus | 0.78 |
| Orinoco | 1.01 |
| Mekong | 1.87 |
| Congo | 2.15 |
| Niger | 3.49 |

*von Eynatten et al. 2003, Math. Geol. 35*

Observed trends often due not correlate with predicted trends

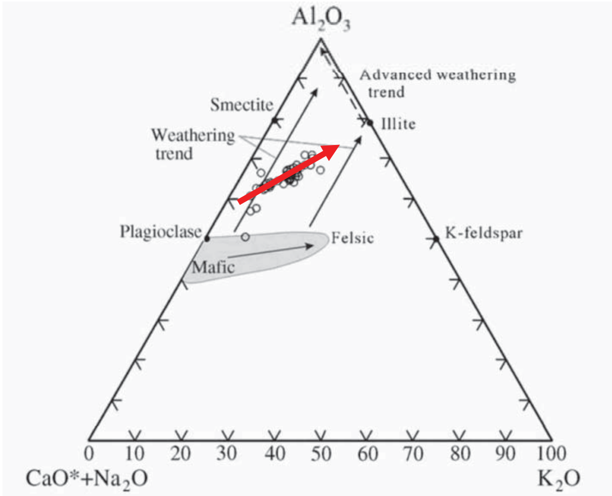


*She et al. 2006, Chem Geol.*

superposition of processes

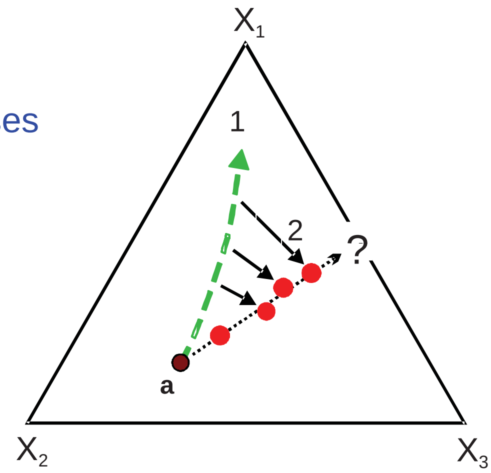


*von Eynatten 2004, Sed Geol*



Trace elements such as Rb, Ba, Sr, U, Th, Zr, etc. may provide valuable additional information on weathering processes

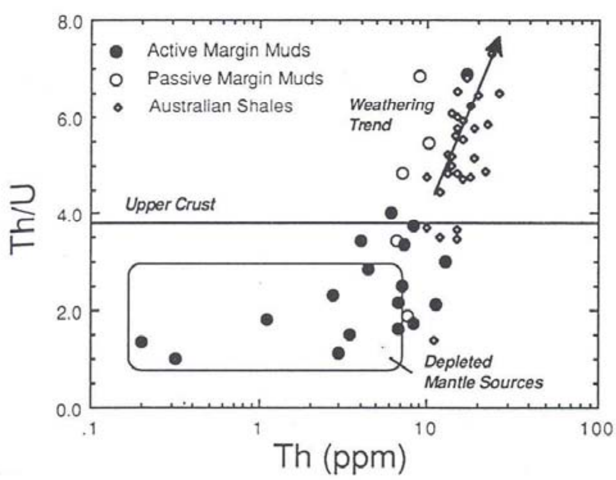


*McLennan 1993*